Reprinted from The Journal of Physical Chemistry, 1994, 98.

Phase Behavior of Two-Component Self-Assembled Monolayers of Alkanethiolates on Gold[1]

John P. Folkers, Paul E. Laibinis, and George M. Whitesides*

Department of Chemistry, Harvard University, Cambridge, Massachusetts 02138

John Deutch*

Department of Chemistry, Massachusetts Institute of Technology, Cambridge, Massachusetts 02139

*Received: May 17, 1993; In Final Form: September 14, 1993**

This paper examines the relationship between the composition of two-component self-assembled monolayers (SAMs) of alkanethiolates on gold and the composition of the solutions from which they were formed. The SAMs were prepared by competitive adsorption of a long-chain alkanethiol ($HS(CH_2)_{21}CH_3$) and a short-chain alkanethiol ($HS(CH_2)_{11}OH$) from solutions in ethanol. Under conditions in which the alkanethiolates in a SAM and the alkanethiols in solution are close to equilibrium, the relationship between the composition of the solution and the composition of the SAM suggests that the monolayer tends, thermodynamically, to exist as a single phase predominantly composed of either long-chain or short-chain thiolates. A derivation of the thermodynamic relationship between the compositions of the SAM and solution is described that includes intermolecular interactions between components in the SAM; theory and experiment agree qualitatively. This analysis concludes that, for a two-component system of alkanethiolates on gold well-equilibrated with alkanethiols in solution, a single phase is preferred at equilibrium; phase-separated, two-component monolayers of the sort extensively studied in Langmuir systems are not observed.

Introduction

"Mixed SAMs" on gold—self-assembled monolayers (SAMs) comprising two alkanethiolates prepared by co-chemisorption from a solution containing two alkanethiols—are useful in studying phenomena involving organic surfaces.[2-13] A number of techniques can establish the *average* composition of a mixed SAM.[2-11] X-ray photoelectron spectroscopy, XPS, can ascertain the composition over an area the size of the X-ray spot (approximately 1 mm^2), and scanning electron microscopy can sometimes detect heterogeneities in composition of a SAM on the dimension of the order of 1 μm;[14] phase separation has not been observed on these scales. In short, neither has the extent to which the components of a mixed SAM segregate into separate phases *within* a SAM been established nor has the question of the relationship between the composition of the solution used to form the SAM and its heterogeneity been addressed experimentally or theoretically. The problem is a difficult one experimentally, because there are few techniques well adapted for direct visualization of phase-separated regions with small sizes in an organic monolayer, especially on optically opaque substrates. Scanning probe microscopies (especially atomic and lateral force microscopies)[17] are techniques that are applicable but only to certain types of SAMs.[17-19]

In this paper, we investigate the phase behavior of two-component SAMs from both theoretical and experimental perspectives. The approach we have taken is thermodynamic—to search for characteristic signatures of phase separation in the dependence of average composition on temperature, concentration, and time—rather than spectroscopic and based on imaging. We focused on the question of whether two-component SAMs form phase-separated domains. In the theoretical section, we derive a thermodynamic relationship between the composition of the solution and the composition of the SAM in terms of interactions between nearest neighbors within the SAM. This relationship predicts that phase separation in a SAM by a mechanism involving the equilibrium of species in the SAM with those in solution will be detectable through a sharp transition between the properties characteristic of one monolayer to those characteristic of the second.

In the Experimental Section, we generate two-component SAMs from $HS(CH_2)_{21}CH_3$ (abbreviated Lg for "long") and $HS(CH_2)_{11}OH$ (Sh for "short") under various experimental conditions. We chose to study SAMs derived from these components because previous qualitative interpretations of experimentally determined relationships between the composition of the mixed SAMs and the composition of the corresponding solutions suggested that mixing of these two components was unfavorable within the SAM.[3,4] In this study, we aimed to determine what the relationship between the composition of the SAMs and the composition of the corresponding solutions would be at equilibrium (if we could indeed reach equilibrium with these components) and to compare this relationship to the theoretically determined relationship. The compositions of the SAMs we have formed in this study span the range from kinetically determined to nearly thermodynamically determined.

The spatial distribution of two thiolates in a mixed SAM cannot be easily determined,[3-5,16] although scanning probe microscopies have suggested, under some conditions, the existence of phase-separated domains.[18] The experiments in this paper are focused on systems consisting of SAMs in equilibrium with solutions containing the corresponding thiols; they do not define the spatial distributions of thiolates in SAMs that are *not* at equilibrium. This work also does not present experimental conditions that guarantee that equilibrium is reached in these systems. We believe, however, that under certain conditions the monolayers do approach equilibrium.

From this work, we conclude that, when at equilibrium with a solution containing a mixture of two components, a SAM will, in general, comprise a single phase and will not consist of regions of separate phases. This single phase may contain one alkanethiolate or a homogeneous mixture of both alkanethiolates. The strength of the interaction between molecules will be the primary factor in determining the composition of that phase.

When mixing of the two components in the SAM is unfavorable, a mixed SAM that is caused to equilibrate at constant composition—that is, when the SAM is not in contact with the solution—could presumably form phase-separated islands. We have not considered this case.

* Abstract published in *Advance ACS Abstracts*, November 1, 1993.

0022-3654/94/2098-0563$04.50/0

Background

Self-assembled monolayers obtained by the adsorption of long-chain alkanethiols (general formula: $HS(CH_2)_nX$, where X is the terminal functional group, or so-called "tail group") onto gold[20] and silver[2,20,21] are useful model systems with which to study the chemistry and properties of organic surfaces. These monolayers are highly ordered;[5,13,20,22-24] the tail groups are exposed at the monolayer–air interface and strongly influence the properties of the interface.[2-13,20,21,23,24] Formation of SAMs from a single thiol allows a limited degree of control over the properties of a surface by choosing the tail group X; formation of SAMs from two thiols allows a greater degree of control over these properties, as both the tail groups and the composition of the SAM can be chosen.[2-12,21] Understanding the phase behavior of two-component self-assembled monolayers is important in interpreting studies of wetting[2-9,13] and adhesion (and perhaps studies of other areas such as protein adsorption)[8] using two-component SAMs.

In Langmuir monolayers, where lateral diffusion allows for equilibration of the system,[25] phase separation has been observed for both single- and two-component monolayers.[26,27] Microscopic phase separation has been predicted theoretically for mixed SAMs derived from alkanethiols with lengths of the alkane chains different by 10 methylene groups, under the assumption that lateral diffusion occurs in the plane of the monolayer and that the composition of the monolayer is fixed.[15] It is not established that either assumption can be realized experimentally;[28,29] the second assumption, in particular, does not apply to the present study.

A recent study using a scanning tunneling microscope (STM) has inferred the existence of phase-separated domains within two-component SAMs formed from solutions containing $HS(CH_2)_{15}CH_3$ and $HS(CH_2)_{15}CO_2CH_3$, although the exact molecular compositions of the domains have not been established.[18] These SAMs were formed from solutions of ethanol with a total concentration of 1 mM in thiol for 4 days at room temperature. A previous study using polarized infrared external reflectance spectroscopy also suggested the existence of domains within mixed SAMs of long- and short-chain alkanethiolates.[5,30] From studies on the rates of exchange between long-chain thiolates in the SAM and similar thiols in solution,[10,21] together with the conclusions from the theoretical section of the present paper, we believe that SAMs that were shown to contain domains but were formed from (and allowed to equilibrate in contact with) solutions containing long-chain alkanethiols at room temperature probably were not at equilibrium with their contacting solutions.

The establishment of equilibrium with mixed SAMs is complicated by at least two types of equilibria: (i) equilibrium *within* a SAM containing two components at fixed composition and (ii) equilibrium *between* a SAM and a solution containing thiol(s). We cannot presently define conditions necessary to achieve equilibrium, because the mechanisms and rates for formation of a monolayer and for exchange of thiolates in a SAM with thiols in solution are not completely known.

Several studies on the kinetics of exchange between long-chain thiolates in a SAM and similar thiols in solution have reached the same general conclusion: at room temperature, exchange is slow, dependent on the concentration of thiol in solution (but not dependent enough to be first order in thiol) and strongly influenced by defect sites within the monolayer (or on the surface of the gold substrate).[10,21,31-33] These results imply that part of the surface structure is "quenched" and that thermodynamic equilibrium in these SAMs at room temperature is approached only slowly after prolonged exposure to solutions with high concentrations of thiol.

In this study, we have varied the experimental conditions used to form SAMs in order to study systems having different relationships between the composition of the SAM and the composition of the solution with which it is in contact. Most, if nct all, of these SAMs—especially those formed at room temperature—have not reached equilibrium, because exchange between thiols in solution and thiolates on the surface is slow.[10,21] We emphasize that the SAMs described here were formed in contact with solutions containing the corresponding thiols. We have no evidence for any type of equilibration within the SAM in the absence of a contacting solution of thiol(s),[28,29] although recent scanning probe studies imply the existence of some lateral mobility of both surface gold atoms[34] and alkanethiolates.[35] We have not examined the influence of the topology of the gold surface on the rates and positions of equilibria.

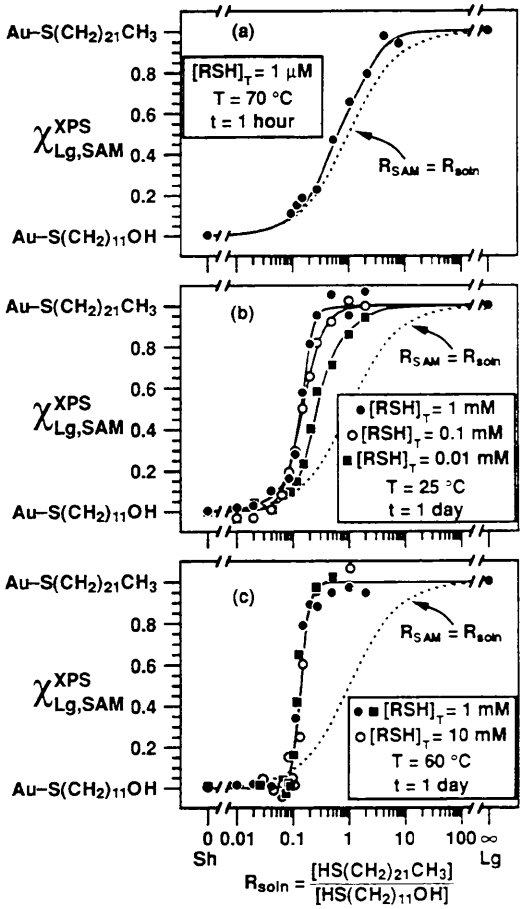

Figure 1. Data for mixed SAMs derived from $HS(CH_2)_{21}CH_3$ and $HS(CH_2)_{11}OH$ adsorbed onto gold from ethanolic solutions. Experimental conditions for the individual experiments are listed in the figure, where $[RSH]_T$ is the total concentration of thiol in solution: (a) data for SAMs closest to ideal or purely kinetic behavior ($R_{SAM} = R_{soln}$); (b) data for SAMS between ideal behavior and equilibrium, showing the progression toward equilibrium as $[RSH]_T$ is increased; (c) data for SAMs closest to equilibrium. Data are plotted as the mole fraction of the longer component in the SAM ($\chi^{XPS}_{Lg,SAM}$, determined from the Au(4f) X-ray photoelectron signal) against the ratio of the concentrations of the two thiols in solution. Some data may have values of $\chi^{XPS}_{Lg,SAM} < 0$ or $\chi^{XPS}_{Lg,SAM} > 1$ because of uncertainties in the measurements: the uncertainty in the intensity of the Au(4f) photoelectron signal usually varies by about ±5%. We have left these data outside the range $\chi^{XPS}_{Lg,SAM} = 0$ and $\chi^{XPS}_{Lg,SAM} = 1$ (rather than moving them to the end points) to show the error in the measurements. The dashed curves represent the mole fraction of the SAM if the composition of a SAM were the same as that of the corresponding solution (denoted by $R_{SAM} = R_{soln}$ in the plot). Lines through the data are presented as guides to the eye.

Results

Analysis of the Composition of the SAMs: Composition of the SAM as a Function of the Composition of the Solution. Figure 1 summarizes the range of relationships between the composition of the SAM and the composition of the solution that we have observed when forming mixed SAMs from ethanolic solutions containing $HS(CH_2)_{21}CH_3$ and $HS(CH_2)_{11}OH$. The data are plotted as the mole fraction of the longer component in the SAM

($\chi_{Lg,SAM} = [Lg]_{SAM}/([Lg]_{SAM} + [Sh]_{SAM})$) as determined using XPS (see the Experimental Section for the method of determining $\chi_{Lg,SAM}$ using XPS) against the ratio of the concentrations of the two thiols in solution ($R_{soln} = [Lg]_{soln}/[Sh]_{soln}$). The dashed curve in each of the plots represents the case where the ratio of the concentrations of the two thiolates in the SAM is the same as that of the two thiols in the corresponding solution; we refer to this case as "$R_{SAM} = R_{soln}$".

In Figure 1a, $R_{SAM} \approx R_{soln}$, although the monolayers are only about 60–70% complete.[36] The low concentration (total concentration of thiol in solution, $[RSH]_T = [HS(CH_2)_{11}OH] + [HS(CH_2)_{21}CH_3] = 1\ \mu M$) and short immersion time ($t = 1$ h) limit the amount of exchange that occurs between thiolates on the surface and thiols in solutions.[37]

In Figure 1c, $R_{SAM} \neq R_{soln}$. The high concentration of thiol ($[RSH]_T = 1$ or 10 mM), long exposure time ($t = 1$ day), and high temperature ($T = 60$ °C) in these experiments accelerate the rate of exchange between thiolates in the SAM and thiols in solution and permit the system to approach equilibrium. We propose that the shape of this curve—an abrupt transition between $\chi_{Lg,SAM} \approx 0$ and $\chi_{Lg,SAM} \approx 1$,[38,39] that is, a transition between SAMs consisting predominantly of either component over a small change in the value of R_{soln}—is characteristic of the tendency of these systems to exist in a single phase at equilibrium, rather than as phase-separated islands.

We can form SAMs from these components for which the relationships between R_{SAM} and R_{soln} are intermediate between these extremes by varying the experimental conditions (Figure 1b). As $[RSH]_T$ is decreased,[40] the composition of the SAM becomes increasingly similar to the composition of the solution; the sharpness of the transition region also decreases with decreasing $[RSH]_T$. The curve for $[RSH]_T = 1$ mM, 25 °C, 1 day is important because it represents the conditions most commonly used in experimental preparation of mixed SAMs.[2-10] The compositions of mixed SAMs thus depend on the conditions under which the adsorptions are performed.

Effect of Phase Structure within a SAM on Its Wettability. We measured the contact angles of water on the mixed SAMs as a function of the conditions for their formation and did not observe any obvious correlation between the wettabilities of the mixed SAMs and the nearness of the SAMs to equilibrium (Figure 1 in the supplementary material shows relevant information). For all of the sets of data, the receding angle of water is practically linearly related to the composition of the SAM, regardless of the experimental conditions under which the SAM was made.[4,41] Using a single set of gold substrates to reduce the variation in the roughnesses of the substrates, we observed that the hysteresis[42] between the advancing and receding contact angles of water on the mixed SAMs increased as the total concentration of thiol was increased in the solution, and thus, as the system moved closer to equilibrium (Figure 2 of the supplementary material). This trend can be rationalized by an increase in the "patchiness" of the SAM as it goes toward equilibrium.[42,43]

Composition of the SAMs Formed at 60 °C as a Function of the Time in Contact with Solution. In Figure 2, we show the effect of long and short times of immersion on the composition of SAMs formed at 60 °C from solutions of ethanol with $[RSH]_T = 1$ mM. These data demonstrate that the compositions of the SAMs do not change considerably by increasing the time in solution beyond 1 day, although the transition region does sharpen on going from 18 h to 5 days.

Figure 2 also shows that considerable exchange between components in solution and components on the surface occurs before the monolayer has completely formed. The open circles in this figure represent SAMs formed for 3 s. Although these monolayers had not formed completely in 3 s (approximately 80% complete by XPS), the relationship between the composition of the SAM and the composition of the solution deviates significantly from $R_{SAM} = R_{soln}$. We do not know whether this exchange occurs during a physisorbed state of the thiols or at the

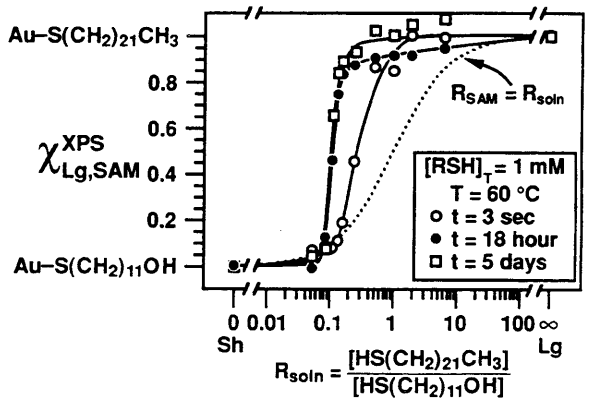

Figure 2. Data for the "kinetics" of adsorption at 60 °C in ethanolic solutions with $[RSH]_T = 1$ mM. Closed circles: SAMs formed after being immersed for 18 h. Open circles: incomplete monolayers formed after being immersed for 3 s. Open squares: SAMs formed after being immersed for 5 days.

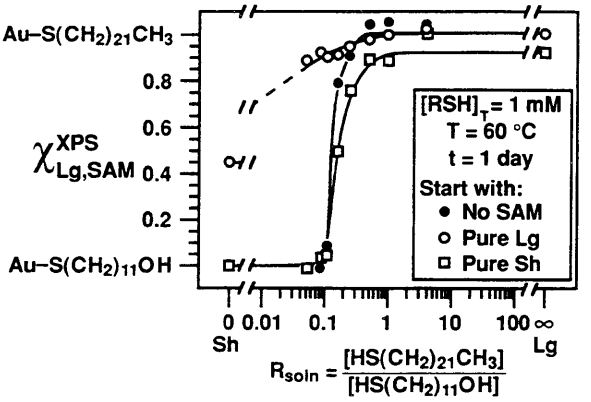

Figure 3. Data for exchange experiments in ethanolic solutions at 60 °C for 1 day with $[RSH]_T = 1$ mM. Closed circles: formation of mixed SAMs on underivatized gold substrates. Open circles: gold substrates with a monolayer derived from $HS(CH_2)_{21}CH_3$ after exchange with a solution of a mixture of thiols with composition given by R_{soln}. Open squares: gold substrates with a monolayer derived from $HS(CH_2)_{11}OH$ after exchange with a solution of a mixture of thiols with composition given by R_{soln}.

state of chemisorbed thiolates in incomplete monolayers (systems in which exchange is probably more rapid than in complete monolayers, due to the lack of lateral stabilization between molecules in the incomplete SAM).

Exchange in Complete SAMs of These Components After 1 Day at 60 °C with $[RSH]_T = 1$ mM. To clarify the rates of exchange between thiolates in SAMs and thiols in solution, we have qualitatively explored exchange reactions at 60 °C starting from different initial points (Figure 3): single-component SAMs derived from $HS(CH_2)_{11}OH$ and $HS(CH_2)_{21}CH_3$ were immersed in ethanolic solutions containing different mixtures of the thiols with $[RSH]_T = 1$ mM at 60 °C for 1 day, and the compositions were compared to those of SAMs formed on underivatized gold. These results demonstrate that removal of the longer component from a SAM is considerably slower than removal of the shorter component. It also shows that even a SAM of the shorter component—the easier component to remove from the SAM by exchange—is not completely removed by the longer component over the length of time used to form the SAMs in Figure 1c (at least for $[RSH]_T = 1$ mM): approximately 10% of the original SAMs seems to survive exchange under these conditions after 1 day.

Thermodynamic Basis for the Phase Behavior in SAMs

We derive a relationship between the mole fraction of the longer thiolate in the SAM (χ_{Lg}) and the ratio of the two thiols in solution (R_{soln}) based on Bragg–Williams solution theory.[44,45] In this derivation, we only include interactions between nearest neighbors.

SCHEME I: Pictorial Representation of the Reference and Mixed States Used To Derive the Interaction Parameter

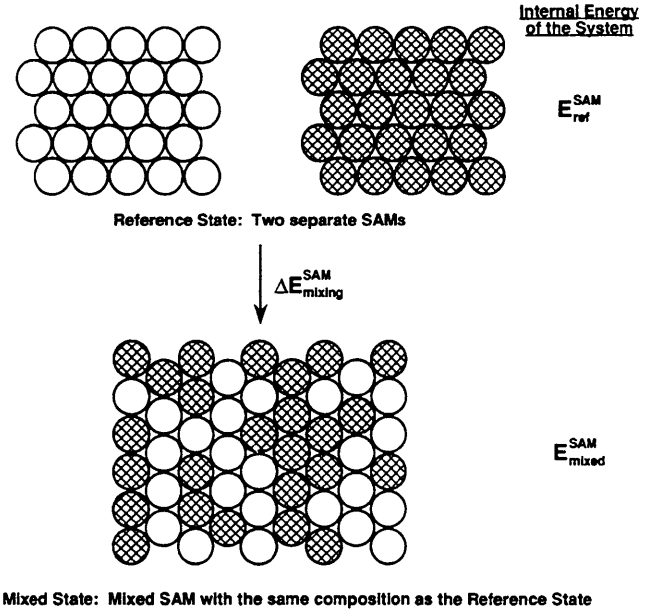

We assume that the thiols in solution are dilute and not interacting. For simplicity, we will also assume that the thiolates have no internal structure, or more precisely, that the internal structure of the adsorbates is the same whether in solution or in a SAM. This assumption does not correspond closely to reality in these conformationally flexible systems, but it does not limit the utility of the treatment.

Thermodynamic Relationship between χ_{Lg} and R_{soln}. This theory describes the change of state on forming mixed SAMs from solution (eq 1).

$$Lg_{soln} + Sh_{soln} \rightarrow Lg_{SAM} + Sh_{SAM} \quad (1)$$

The chemical potential of a thiol in solution is

$$\mu_i^{soln} = \mu_i^{\dagger} + kT \ln y_i \quad (2)$$

where i is either Lg or Sh, y_i is the mole fraction of the thiol in solution ($y_{Lg} + y_{Sh} \neq 1$ because of the mole fraction of the solvent; $y_{Lg}/y_{Sh} \equiv R_{soln}$),[46] $\mu_i^{\dagger}$ is the chemical potential of the thiol when it is at infinite dilution ($y_i \rightarrow 0$),[47] k is Boltzmann's constant, and T is the absolute temperature of the system. The chemical potential of a thiolate in the mixed SAM is

$$\mu_i^{SAM} = \mu_i^{*} + kT \ln \chi_i + \varpi(1 - \chi_i)^2 \quad (3)$$

where μ_i^{*} is the chemical potential of the thiolate in the single-component SAM, χ_i is the mole fraction of the thiolate in two-component SAM (in the SAM, $\chi_{Lg} + \chi_{Sh} \equiv 1$),[46] and ϖ is the interaction parameter, which describes intermolecular interactions within the SAM.

The interaction parameter is derived from the difference in internal energy between a two-component or "mixed" SAM (E^{SAM}_{mixed}, eq 4) and two separate, single-component SAMs (E^{SAM}_{ref}, eq 5)—that is, the reference state (see Scheme I). In eqs 4 and 5,

$$E^{SAM}_{mixed} = [\omega_{LgLg}N^{SAM}_{LgLg} + \omega_{ShSh}N^{SAM}_{ShSh} + \omega_{LgSh}N^{SAM}_{LgSh}] \quad (4)$$

$$E^{SAM}_{ref} = (Z/2)[\omega_{LgLg}N^{SAM}_{Lg} + \omega_{ShSh}N^{SAM}_{Sh}] \quad (5)$$

ω_{ij} is the interaction energy between the molecules i and j (positive values of ω_{ij} correspond to repulsive interactions), N^{SAM}_{ij} is the number of nearest-neighbor interactions of a specific type within the SAM, and N^{SAM}_{i} is the number of molecules of the type i in the SAM. In the Bragg–Williams approximation, $N^{SAM}_{ii} = ZN^{SAM}_{i}\chi_i/2$ and $N^{SAM}_{ij} = ZN^{SAM}_{i}\chi_j = ZN^{SAM}_{j}\chi_i$, where Z is the number of nearest neighbors. Using these relationships, we obtain

$$e^{SAM}_{mixed} = (Z/2)[\omega_{LgLg}(\chi_{Lg})^2 + \omega_{ShSh}(\chi_{Sh})^2 + 2\omega_{LgSh}\chi_{Lg}\chi_{Sh}] \quad (6)$$

from eq 4 and

$$e^{SAM}_{ref} = (Z/2)[\omega_{LgLg}\chi_{Lg} + \omega_{ShSh}\chi_{Sh}] \quad (7)$$

from eq 5, where energy is presented as the energy per molecule: $e = E/(N^{SAM}_{Lg} + N^{SAM}_{Sh})$. The change in internal energy on going from two separate, single-component monolayers to a mixed monolayer is

$$\Delta e^{SAM}_{mixing} = e^{SAM}_{mixed} - e^{SAM}_{ref} = (Z/2)[2\omega_{LgSh} - \omega_{LgLg} - \omega_{ShSh}]\chi_{Lg}\chi_{Sh} \quad (8)$$

and we define the interaction parameter ϖ as

$$\varpi = (Z/2)[2\omega_{LgSh} - \omega_{LgLg} - \omega_{ShSh}] \quad (9)$$

We now determine the change in Gibbs free energy for the formation of a mixed SAM (Δf). The general equation for forming a SAM composed of χ_{Lg} and χ_{Sh} mole fractions of the long and short thiolates, respectively, is

$$\Delta f = \chi_{Lg}(\mu^{SAM}_{Lg} - \mu^{soln}_{Lg}) + \chi_{Sh}(\mu^{SAM}_{Sh} - \mu^{soln}_{Sh}) \quad (10)$$

When we insert the definitions of the chemical potentials for thiols in solution and thiolates in the SAM (as given in eqs 2 and 3, respectively), we obtain

$$\Delta f = \chi_{Lg}(\mu_{Lg}^{*} - \mu^{\dagger}_{Lg}) - \chi_{Lg}kT \ln y_{Lg} = \chi_{Sh}(\mu_{Sh}^{*} - \mu^{\dagger}_{Sh}) - \chi_{Sh}kT \ln y_{Sh} + \Delta f^{SAM}_{mixing} \quad (11)$$

where the free energy of mixing of the components in the SAM is

$$\Delta f^{SAM}_{mixing} = kT(\chi_{Lg} \ln \chi_{Lg} + \chi_{Sh} \ln \chi_{Sh}) + \varpi\chi_{Lg}\chi_{Sh} \quad (12)$$

The first term in eq 12 is the entropy of mixing; the second term is the internal energy of mixing from eq 8. Strictly speaking, for Gibbs free energy, the second term in eq 12 should be the enthalpy of mixing, not the internal energy of mixing. The difference between these quantities involves contributions from the equation of state of the SAM that are unknown for these systems. Since we have assumed structureless particles confined to sites on a lattice, we can assume that these terms will be negligible as long as the monolayers are complete;[48] we therefore neglect the difference between enthalpy and internal energy in our treatment.

No Mixing between Components in the SAM. If we consider a system where absolutely no mixing of the two components occurs, we obtain the change in free energy for the formation of the SAM:

$$\Delta f = \chi_{Lg}(\Delta(\Delta\mu) - kT \ln R_{soln}) + (\mu_{Sh}^{*} - \mu^{\dagger}_{Sh}) - kT \ln y_{Sh} \quad (13)$$

where

$$\Delta(\Delta\mu) = \Delta\mu_{Lg} - \Delta\mu_{Sh} = (\mu_{Lg}^{*} - \mu^{\dagger}_{Lg}) - (\mu_{Sh}^{*} - \mu^{\dagger}_{Sh}) \quad (14)$$

To determine the relationship between R_{soln} and χ_{Lg}, we minimize the free energy with respect to χ_{Lg}: if $kT \ln R_{soln} < \Delta(\Delta\mu)$, then the free energy will be a minimum when $\chi_{Lg} = 0$; if $kT \ln R_{soln} > \Delta(\Delta\mu)$, then the free energy will be a minimum when $\chi_{Lg} = 1$. For this system, a plot of χ_{Lg} against $\ln R_{soln}$, therefore, will be discontinuous at $\ln R_{soln} = \Delta(\Delta\mu)/kT$ (Figure 4).

Mixing between Components in the SAM. Determination of the relationship between χ_{Lg} and R_{soln} becomes more complex when we allow the two components to mix in the SAM. In this case, we minimize eq 11 with respect to the mole fraction of the

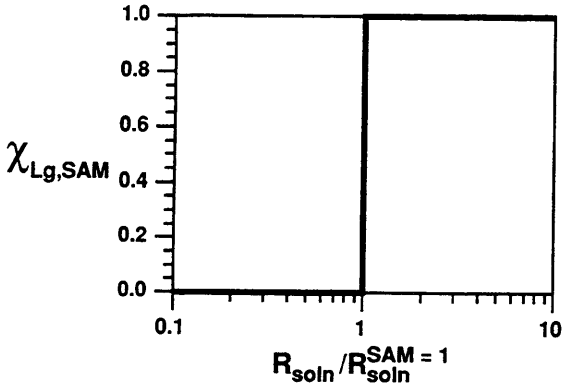

Figure 4. Theoretical relationship between R_{soln} and χ_{Lg} when no mixing between the components occurs. The x-axis is plotted as the ratio of R_{soln} to $R_{soln}^{SAM=1}$; $R_{soln}^{SAM=1}$ is the value of R_{soln} that yields equimolar quantities of the two thiolates in the SAM.

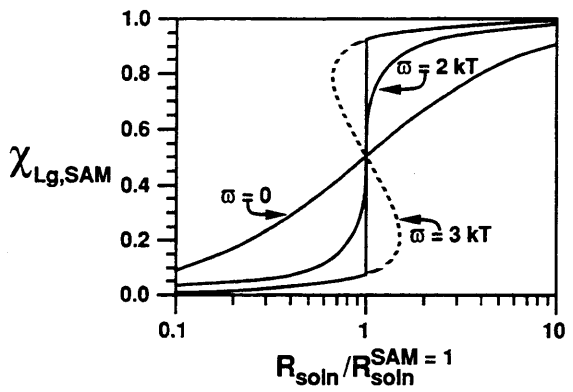

Figure 5. Theoretical relationships between R_{soln} and χ_{Lg} determined using eq 16. Three values of the interaction parameter ϖ are shown corresponding to well-mixed SAMs ($\varpi = 0$), SAMs with critical mixing ($\varpi = 2kT$), and SAMs in which mixing of the components is not favored ($\varpi = 3kT$). The plot of χ_{Lg} against R_{soln} for $\varpi = 3kT$ shows the equilibrium relationship corresponding to the minimum energy phases (solid line) and the calculated relationship corresponding to metastable states (dashed curve). The minimum was determined using eq 11 and the method described in the text. The x-axis is plotted as the ratio of R_{soln} to $R_{soln}^{SAM=1}$.

longer component in the SAM,

$$d(\Delta f)/d\chi_{Lg} = 0 = \Delta(\Delta\mu)/kT - \ln R_{soln} + \ln(\chi_{Lg}/(1-\chi_{Lg})) + (\varpi/kT)(1-2\chi_{Lg}) \quad (15)$$

After rearrangement, we obtain

$$R_{soln}\exp(-\Delta(\Delta\mu)/kT) = (\chi_{Lg}/(1-\chi_{Lg}))\exp((\varpi/kT)(1-2\chi_{Lg})) \quad (16)$$

as the relationship between R_{soln} and χ_{Lg}. We plot our results as the logarithm of R_{soln} against χ_{Lg}:

$$\ln R_{soln} = \ln(\chi_{Lg}/(1-\chi_{Lg})) + (\varpi/kT)(1-2\chi_{Lg}) + \Delta(\Delta\mu)/kT \quad (17)$$

The two unknowns in these equations are $\Delta(\Delta\mu)$ and ϖ; R_{soln} is the experimentally controlled parameter, and χ_{Lg} is the experimentally measured parameter.

If $R_{soln} = 1$, the quantity $\Delta(\Delta\mu)/kT$ is related to the shift of χ_{Lg} from $\chi_{Lg} = 0.5$ and reflects the preference of one component over the other in the SAM relative to the solution. When $\Delta(\Delta\mu) > 0$, the center of the transition region (where $\chi_{Lg} = 0.5$) will occur at values greater than $R_{soln} = 1$; in this case, the driving force for having the shorter component *on the surface* relative to having it in solution is greater than that for the longer component. When $\Delta(\Delta\mu) < 0$, the center of the transition region will shift to values less than $R_{soln} = 1$; the longer component is favored on the surface. It is important to remember that $\Delta(\Delta\mu)$ is independent of the interaction parameter in this derivation and is only dependent on the standard-state chemical potentials of the molecules in the solution and in the SAM (see eq 14). In this paper, we will refer to the quantity $\exp(\Delta(\Delta\mu)/kT)$ as $R_{soln}^{SAM=1}$: it is the value of R_{soln} that yields equimolar quantities of the two thiolates in the SAM (i.e., the value of R_{soln} for which $R_{SAM} = 1$ at equilibrium).[49]

Analysis of the Interaction Parameter ϖ. In this section, we give a physical interpretation of values of ϖ in units of kT. The value of the interaction parameter will determine the phase behavior of the SAMs.

To interpret ϖ, we determine the number of singular points, $d \ln R_{soln}/d\chi_{Lg} = 0$ (or $d\chi_{Lg}/d \ln R_{soln} = \infty$ in the way we plot our data), in the relation between $\ln R_{soln}$ and χ_{Lg} (eq 17). We find the singular points $\chi_{Lg}^{\pm}$ from eq 18.

$$\chi_{Lg}^{\pm} = {}^1/_2 \pm {}^1/_2(1-2kT/\varpi)^{1/2} \quad (18)$$

There are three regimes defined by values of ϖ. For simplicity, we rewrite eq 17 as eq 19,

$$\ln(R_{soln}/R_{soln}^{SAM=1}) = \ln(\chi_{Lg}/(1-\chi_{Lg})) + (\varpi/kT)(1-2\chi_{Lg}) = \phi(\chi_{Lg}) \quad (19)$$

(1) When $\varpi < 2kT$, a plot of χ_{Lg} versus $\phi(\chi_{Lg})$ increases monotonically in the region $0 < \chi_{Lg} < 1$; a particular value of $\ln(R_{soln}/R_{soln}^{SAM=1})$ equals $\phi(\chi_{Lg})$ at only a single value of ϖ (see, for example, Figure 5 for $\varpi = 0$). (2) When $\varpi = 2kT$, there is exactly one singular point at $\chi_{Lg}^{+} = \chi_{Lg}^{-} = 0.5$, and the plot of χ_{Lg} versus $\phi(\chi_{Lg})$ becomes vertical at $\chi_{Lg} = 0.5$ (see Figure 5). (3) When $\varpi > 2kT$, the plot of χ_{Lg} versus $\phi(\chi_{Lg})$ becomes multivalued (see $\varpi = 3kT$ in Figure 5 including dashed line), and there are two distinct singular points χ_{Lg}^{+} and χ_{Lg}^{-}. Certain values of $\ln(R_{soln}/R_{soln}^{SAM=1})$ will cross the curve $\phi(\chi_{Lg})$ at these values of χ_{Lg}.

The physical interpretation of the different regions of ϖ are these: (1) When the interaction parameter ϖ is less than zero, then interactions between unlike molecules are more favorable than interactions between like molecules (as might be the case, for example, in a monolayer composed of components containing electron-donor and electron-acceptor groups). When ϖ is equal to zero, then the mixture is ideal: the components are energetically equivalent. When $0 < \varpi < 2kT$, the components prefer to be surrounded by their own kind, but the interaction energy is not sufficient to overcome the entropy of mixing. We, therefore, expect complete mixing when $\varpi < 2kT$. (2) If $\varpi = 2kT$, we have critical mixing of the two components in the SAM. (3) When $\varpi > 2kT$, the plot of χ_{Lg} against $\ln R_{soln}$ shows that over a range of values of R_{soln} centered about the midpoint there are three possible values of χ_{Lg} for each value of R_{soln} (Figure 5). Call the possible values χ_{Lg}^{1}, χ_{Lg}^{2}, and χ_{Lg}^{3}. To determine which composition has the lowest free energy, we must evaluate $\Delta f(\chi_{Lg}^{1})$, $\Delta f(\chi_{Lg}^{2})$, and $\Delta f(\chi_{Lg}^{3})$ from eq 11. For each value of R_{soln}, we determine the candidate value of χ_{Lg} by selecting the value that yields the lowest free energy. The result is displayed in Figure 5 for $\varpi = 3kT$ as the solid line. To simplify these calculations, we have assumed that $\Delta(\Delta\mu) = 0$ (i.e., $\Delta\mu_{Lg} = \Delta\mu_{Sh}$), but the conclusion is the same: the equilibrium relationship between $\ln R_{soln}$ and χ_{Lg} will have a vertical break at the midpoint at $R_{soln} = R_{soln}^{SAM=1}$. The other two compositions (dashed lines in Figure 5) correspond to phases that are metastable; these phases will, therefore, not occur at equilibrium.

In Figure 6, we plot the composition as a function of temperature to show the calculated phase behavior of this system. In this plot, we take an interaction parameter equal to $3kT$ at room temperature ($\varpi = 1.8$ kcal/mol) as a reference point. We present this plot for two reasons: Figure 6 shows the relationship between the interaction parameter and temperature (left and right axes), and it also shows the relationship between the compositions of the most stable phases in the SAM (solid curve) and temperature (and, consequently, the value of the interaction parameter). Note

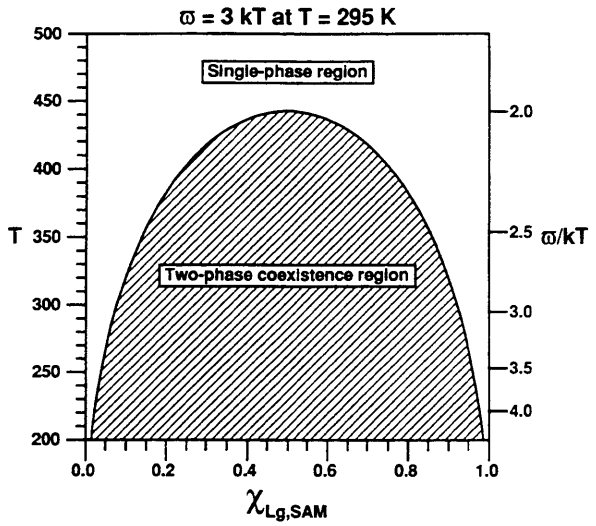

Figure 6. Phase diagram for two-component SAMs if the interaction parameter is equal to $3kT$ at room temperature (ϖ = 1.8 kcal/mol at 295 K). The left side of the plot shows the temperature in kelvin; the right side shows the corresponding interaction parameter.

that the compositions in the area beneath the curve (the lined area) of Figure 6 will never be formed at equilibrium when SAMs are formed from solutions containing an excess of the two thiols.

Discussion

It Is Nearly Impossible to Form a Mixed SAM with Phase-Separated Islands if the SAM Has Reached Equilibrium with a Solution Containing an Excess of the Two Thiols. The most important theoretical conclusion from this paper is that when a mixed SAM is in equilibrium with a contacting solution containing an excess of the two components, two phases will coexist in that SAM *only if* $R_{soln} = R_{soln}^{SAM=1}$ *and* $\varpi > 2kT$; for all other values of R_{soln}—regardless of the value of ϖ—only one phase will exist in the SAM at equilibrium. When ϖ is greater than the critical value, the predicted range of values of R_{soln} that will permit the existence of phase-separated domains is so narrow as to be experimentally unachievable. At equilibrium, formation of phase-separated SAMs over a wide range of values for R_{soln}, therefore, suggests that the SAMs have not reached equilibrium.

Two-component Langmuir monolayers can contain a mixture of two phases because the composition of the monolayer can be controlled exactly and fixed[27] and because the mechanism of equilibration is lateral diffusion of the components in the plane of the monolayer.[25] Two-component SAMs could similarly form two phases if they were isolated from a thiol-containing solution and if lateral diffusion occurred by some mechanism.[28,29] In SAMs, the composition is determined by the interactions within the SAM; since the solution generally contains an excess of each component, only a single-phase SAM will result at equilibrium.

Are the Mixed SAMs in Figure 1 at Equilibrium? From previous studies dealing with the kinetics of exchange in complete monolayers,[10,21] we conclude that mixed SAMs formed from ethanolic solutions containing $HS(CH_2)_{21}CH_3$ and $HS(CH_2)_{11}OH$ *at room temperature are not at equilibrium*, because exchange between thiolates in the SAM and thiols in solution is slow and incomplete at room temperature.[10,21] Mixed SAMs are often formed at room temperature; we infer that none of these SAMs are at equilibrium.

SAMs formed at temperatures higher than room temperature (for the studies in this paper, $T \geq 60$ °C) from solutions with high values of $[RSH]_T$ are probably closest to equilibrium. The SAMs in Figure 1a are, however, not at equilibrium because of the short immersion time and the low concentration of thiol.[37] The results in Figure 1a correspond to kinetically trapped, metastable compositions.

One result that suggests that the SAMs in Figure 1c may be close to equilibrium compositions is that the relationship between χ_{Lg} and R_{soln} is nearly the same whether the SAMs were formed from solutions with $[RSH]_T$ = 1 mM or from solutions with $[RSH]_T$ = 10 mM. This result suggests either that the monolayers have reached stable compositions or that the exchange rate is not dependent on the concentration of thiol in solution. At room temperature, the rate-limiting step of exchange between thiols in solution and thiolates in a SAM is predominantly desorption of species from the surface, although there is still a significant (although less than first-order) dependence of the rate of exchange on the concentration of thiol in solution at room temperature.[10] We have also observed a dependence of the rate of exchange on the concentration of thiol in solution at 60 °C.[50] (We note that, even after long times of exchange, there could be molecules within the SAMs that have not exchanged; kinetically trapped thiolates have been observed in SAMs at room temperature.[10])

The results in Figures 2 and 3 suggest also that the SAMs in Figure 1c (at least those for $[RSH]_T$ = 1 mM) are close to, but probably have not fully reached, equilibrium. In Figure 2, only a small change in the sharpness of the transition region was observed on changing the time in solution from 18 h to 5 days for SAMs at 60 °C. Figure 3 shows the thiols in solution do not exchange completely with thiolates in a complete SAM after 1 day at 60 °C with $[RSH]_T$ = 1 mM.

Recent Studies Have Suggested the Existence of Phase-Separated Domains within Mixed SAMs. In other, independent experiments, we have inferred evidence that SAMs formed under "normal" conditions (room temperature, $[RSH]_T$ = 1 mM, 1 day) consist of regions of different phases.[5] In these experiments, polarized infrared external reflectance spectroscopy (PIERS) was applied to mixed SAMs containing long- and short-chain thiolates formed under normal conditions.[30] The frequencies and relative intensities of the stretching vibrations of the methyl and methylene groups in the molecules indicated that the SAMs contained both regions where the outer parts of the longer chains were in a liquid-like state and regions where these outer parts were in a crystal-like state. The observation of crystalline regions suggests that these SAMs consist, in part, of islands.

The results from the PIERS study are consistent with images of mixed SAMs collected with a scanning tunneling microscope.[18] Several experimental results suggest that the SAMs formed in these studies were not at equilibrium. Exchange between thiolates in the SAM and thiols in solution is slow and incomplete at room temperature and becomes slower as the alkyl group on the thiolate is lengthened.[10] This exchange is slower on gold substrates that are flatter than the normal polycrystalline samples often employed.[33] The effect of the slow exchange could be the formation of islands as the SAM goes toward equilibrium (both with solution and internally).

The nature of these islands, and of the processes that form them, remains undefined. One possibility, suggested by the theoretical conclusion from this work that multiple phases are not likely to coexist at equilibrium, is that the islands represent single-phase, single-component "near-equilibrium" regions in a sea of a different average composition that is initially formed kinetically. The kinetically formed regions could contain mixtures of the two thiolates, and, as a consequence, would be disordered; the "near-equilibrium" regions would be formed where surface features (step, defects, ...) would favor exchange of thiolates in the SAM with thiols in solution.

Conclusions

This study concludes that mixed SAMs formed from the adsorption of a long-chain and a short-chain alkanethiol onto gold, and allowed to equilibrate completely in contact with a solution containing these thiols, will exist as single phases at equilibrium. This single phase may contain both thiolates or predominantly (or exclusively) one, depending on the magnitude

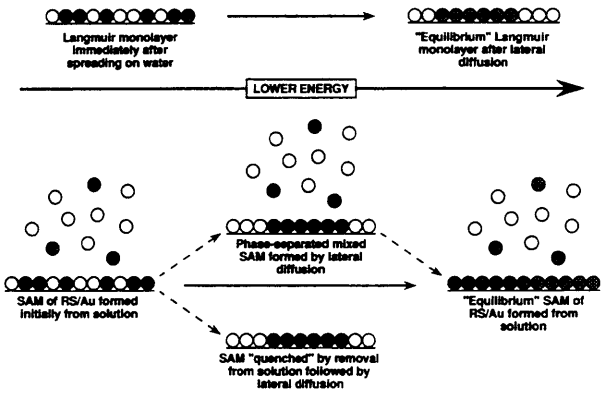

Figure 7. Schematic illustration of the difference between the predominant mechanisms of equilibration in two-component Langmuir monolayers and two-component self-assembled monolayers of alkanethiolates on gold. The top illustrates equilibration in two-component Langmuir films, which occurs by lateral diffusion of the molecules in the plane of the monolayer; note that the composition is not change during equilibration. The bottom illustrates equilibration in two-component self-assembled monolayers of alkanethiolates on gold, which occurs predominantly by exchange with species in solution; note that in solution, the composition of the SAM changes during equilibration. We have implied a large magnitude of ϖ in favor of the darker species for illustrative purposes.

of interactions between "like" and "unlike" pairs of thiolates in the SAM. The important point is that (unlike Langmuir monolayers at the air–water interface) two-component SAMs will not phase separate into islands of different compositions at equilibrium under these conditions.

Since most of our SAMs are not at equilibrium, they may contain two phases: the composition of one phase could be the composition obtained at equilibrium; the composition of the other could be random, but would probably be closer to an initial, kinetically formed composition. As a SAM approaches equilibrium, islands of the equilibrium composition would grow until, at equilibrium, the whole SAM was that composition.

The essential difference between SAMs of alkanethiolates on gold and Langmuir monolayers is the different processes leading toward equilibrium. In a Langmuir monolayer, the overall composition of the monolayer is fixed when it is first spread and does not change thereafter; equilibrium is reached by lateral diffusion, which is fast within the monolayer on the time scale of the experiment (Figure 7).[25] By contrast, SAMs on gold appear to require equilibration with a solution containing alkanethiols, and evidence for any lateral diffusion is still inferential.[35] Thus, for Langmuir monolayers, equilibration reaches an equilibrium state of fixed composition by lateral diffusion; for SAMs, equilibrium is usually approached experimentally by equilibration with an infinite reservoir of thiols. It usually involves a change in composition of the monolayer and does not seem to involve rapid lateral diffusion (see Figure 7). If Langmuir systems could be devised that would equilibrate the monolayer with a solution reservoir containing its components, the analysis developed here should apply to the final equilibrium state; if a method could be found to promote lateral diffusion within an alkanethiolate SAM on gold, it could be removed from contact with its solution reservoir of alkanethiols and would reach an equilibrium with phase-separated islands.

Lateral diffusion of the thiolates could only affect the final distribution of thiolates in a monolayer if the SAM were removed from solution before it had reached equilibrium with the solution. The SAM could then reach an equilibrium distribution analogous to that observed in Langmuir monolayers by way of lateral diffusion. For a SAM in contact with a solution containing thiol, the equilibrium structure will always contain one phase even if lateral diffusion is fast, because no matter what lateral diffusion leads to, the system can lower its energy by becoming a single phase (Figure 7).

An important question that remains unresolved from this work concerns *completely* mixed systems. We have not been able to prepare systems that correspond to kinetically trapped, mixed phases. Although Figure 1a approximates the behavior expected for such as system, the SAMs are incomplete. Why are we *not* able to form complete, mixed SAMs? We suggest that formation of the SAM can be considered to proceed in at least three steps. The first is physisorption of alkanethiols (RSH) on the surface of the gold.[51] Dialkyl sulfides (RSR) adsorb on gold;[52] alkanethiols should also be able to adsorb to gold without breaking the S–H bond.[52] We expect exchange of alkanethiol in solutions with alkanethiol physisorbed on the surface to be relatively fast. The second step is conversion of physisorbed alkanethiol to chemisorbed gold(I) alkanethiolate, with loss of the hydrogen from the thiol (presumably as H_2, although its presence has never been demonstrated experimentally). This step might be expected to be relatively slow. The third step is exchange of alkanethiol in solution with alkanethiolates on the surface. This process might proceed by the microscopic reverse of the first and second steps or by some independent process (such as the desorption of disulfides[51] or the desorption of gold thiolates[43]). Depending on the relative rates of these various processes, it would, in principle, be possible to achieve a range of behaviors connecting the compositiion of the solution and the composition of the monolayer. We infer that the rates of all three steps are comparable, although the third is probably the slowest. In particular, we hypothesize that significant equilibration occurs at the stage of physisorbed thiols, before formation of the chemisorbed thiolates.

Experimental Section

Preparation of Substrates. Gold substrates were prepared by electron-beam evaporation of ~100 Å of chromium (Aesar; 99.99%) followed immediately by evaporation of ~2000 Å of high-purity gold (Materials Research Corp.: Orangeburg, NY; 99.9999%) onto single-crystal silicon (100) test wafers (Silicon Sense: Nashua, NH; 100-mm diameter, ~500 μm thick). Chromium was used as an adhesive layer between the gold and the native oxide on the silicon. The metals were evaporated at a rate of 5 Å/s onto substrates that were not heated.[31] The gold-coated silicon wafers were cut into ~1 cm × 3 cm slides with a diamond-tipped stylus before being put into solution.

Formation of SAMs. Adsorptions were carried out either in 20-mL single-use glass scintillation vials or in 25-mL glass weighing bottles. All adsorptions above room temperature were carried out in glass weighing bottles. Prior to each experiment, the weighing bottles were cleaned with "piranha solution" (7:3 concentrated H_2SO_4/30% H_2O_2) at ~90 °C for 30 min, rinsed with deionized water, and dried in an oven at 200 °C for at least 12 h.

WARNING: Piranha solution should be handled with caution; in some circumstances (most probably when it had been mixed with significant quantities of an oxidizable organic material), it has detonated unexpectedly.[53]

Docosanethiol and 11-mercaptoundecanol were available from previous studies;[2-5] absolute ethanol (Quantum Chemical Corp. or Pharmco Products, Inc.) was used as solvent for all adsorptions and was deoxygenated with N_2 prior to use. Solutions with $[RSH]_T$ = 10 mM were made by weighing the appropriate amount of each thiol into glass weighing bottles. Solutions with $[RSH]_T$ = 0.1 mM or 1 mM were prepared by dilutions of appropriate amounts of docosanethiol and 11-mercaptoundecanol from freshly prepared stock solutions. Solutions with $[RSH]_T$ = 0.01 mM or 1 μM were prepared by dilution of 0.1 mM solutions. Adsorptions at high temperatures were carried out in a temperature-controlled oil bath; the temperature of the oil bath was controlled to within ±1 °C by a Dyna-Sense temperature controller (Cole Parmer). The solutions were equilibrated in the oil bath for at least 2 h before addition of the slides. After removal from solution, the slides were rinsed with ethanol and dried in a stream of N_2.

Characterization of SAMs. All SAMs were characterized using contact angles and X-ray photoelectron spectroscopy (XPS). The apparatus and method for the measurement of contact angles have been described previously.[4,20]

X-ray photoelectron spectra were taken on the same slides as used for the contact angles within several days after removal from solution; slides were stored in wafer trays (Fluoroware) prior to characterization by XPS. Spectra were collected on an SSX-100 spectrometer (Surface Science Instruments) using monochromatic Al Kα X-rays. The "spot size" was either 600 or 1000 μm, and the pass energy on the detector was either 50 or 100 eV. For quantitation of the individual elements in the SAMs, we used the 4f doublet for gold ("Au(4f)" at 84 and 87 eV for $4f_{7/2}$ and $4f_{5/2}$, respectively) and the 1s peaks for carbon and oxygen ("C(1s)" and "O(1s)" at 284 and 532 eV, respectively). Two scans were taken for both gold and carbon, and 10 scans were taken for oxygen (acquisition time for one scan was approximately 2 min). Spectra were fitted using an 80% Gaussian/20% Lorentzian peak shape.

Determination of the Composition of the SAMs Using XPS. To determine the compositions of the mixed SAMs, we used the natural logarithm of the Au(4f) peak because it is directly related to the thickness of the hydrocarbon layer (d_{HC}) of a two-component SAM through eq 21.[54] Equation 21 comes directly from eq 20, which models the inelastic scattering of the photoelectrons

$$\mathrm{Au(4f)_{SAM}} = \mathrm{Au(4f)_0}\beta \exp(-d_{HC}/(\lambda \sin \phi)) \quad (20)$$

$$\ln \mathrm{Au(4f)_{SAM}} = -d_{HC}/(\lambda \sin \phi) + \text{constant} \quad (21)$$

through the hydrocarbon layer as an exponential decay. In these equations, $\mathrm{Au(4f)_0}$ is the intensity of the Au(4f) peaks for a bare gold substrate, β is a term for attenuation due to the sulfur atom on each thiolate, λ is the inelastic mean free path of the photoelectrons through the hydrocarbon layer (40 Å),[54,55] and ϕ is the angle between the plane of the substrate and the detector (35°).

In terms of χ_{Lg}, we write eq 21 as

$$\ln \mathrm{Au(4f)_{SAM}} = -(\chi_{Lg}(d_{Lg} - d_{Sh}) + d_{Sh})/(\lambda \sin \phi) + \text{constant} \quad (22)$$

where d_{Lg} and d_{Sh} are the thicknesses of the hydrocarbon layers for the single-component SAMs. After relating d_{Lg} and d_{Sh} to $\ln \mathrm{Au(4f)_{Lg}}$ and $\ln \mathrm{Au(4f)_{Sh}}$, respectively, using eq 21, and substituting these relationships into eq 22, we obtain

$$\chi_{Lg} = (\ln \mathrm{Au(4f)_{SAM}} - \ln \mathrm{Au(4f)_{Sh}})/(\ln \mathrm{Au(4f)_{Lg}} - \ln \mathrm{Au(4f)_{Sh}}) \quad (23)$$

as the relationship between χ_{Lg} and the experimentally measured quantities.

Acknowledgment. We thank our colleagues Nicholas Abbott, Hans Biebuyck, and Mathai Mammen for useful discussions and comments. Professors David Allara and Paul Weiss of Penn State provided us with a copy of ref 18 and with valuable discussions of phase separation.

Supplementary Material Available: Figure 1 showing plots of advancing and receding contact angles of water and Figure 2 showing the hysteresis between the advancing and receding contact angles of water as a function of the composition of the monolayers for the six sets of SAMs shown in Figure 1 (4 pages). Ordering information is given on any current masthead page.

References and Notes

(1) This research was supported in part by the Office of Naval Research, the Defense Advanced Research Projects Agency. XPS spectra were obtained using instrument facilities purchased under the DARPA/URI program and maintained by the Harvard University Materials Research Laboratory.

(2) Au: Bain, C. D.; Evall, J.; Whiteside, G. M. *J. Am. Chem. Soc.* **1989**, *111*, 7155–7164. Cu, Ag, Au: Laibinis, P. E.; Whitesides, G. M. *J. Am. Chem. Soc.* **1992**, *114*, 1990–1995.

(3) Bain, C. D.; Whitesides, G. M. *J. Am. Chem. Soc.* **1988**, *110*, 3665–3666. Bain, C. D.; Whitesides, G. M. *Science (Washington, D.C.)* **1988**, *240*, 62–63. Bain, C. D.; Whitesides, G. M. *J. Am. Chem. Soc.* **1989**, *111*, 7164–7175.

(4) Folkers, J. P.; Laibinis, P. E.; Whitesides, G. M. *Langmuir* **1992**, *8*, 1330–1341.

(5) Laibinis, P. E.; Nuzzo, R. G.; Whitesides, G. M. *J. Phys. Chem.* **1992**, *96*, 5097–5105.

(6) Bertilsson, L.; Liedberg, B. *Langmuir* **1993**, *9*, 141–149.

(7) Bain, C. D.; Whitesides, G. M. *Langmuir* **1989**, *5*, 1370–1378.

(8) Pale-Grosdemange, C.; Simon, E. S.; Prime, K. L.; Whitesides, G. M. *J. Am. Chem. Soc.* **1991**, *113*, 12–20. Prime, K. L.; Whitesides, G. M. *Science (Washington, D.C.)* **1991**, *252*, 1164–1167.

(9) Ulman, A.; Evans, S. D.; Shnidman, Y.; Sharma, R.; Eilers, J. E.; Chang, J. C. *J. Am. Chem. Soc.* **1991**, *113*, 1499–1506. Sanassy, P.; Evans, S. D. *Langmuir* **1993**, *9*, 1024–1027.

(10) Chidsey, C. E. D.; Bertozzi, C. R.; Putvinski, T. M.; Mujsce, A. M. *J. Am. Chem. Soc.* **1990**, *112*, 4301–4306. Collard, D. M.; Fox, M. A. *Langmuir* **1991**, *7*, 1192–1197.

(11) Hickman, J. J.; Ofer, D.; Laibinis, P. E.; Whitesides, G. M.; Wrighton, M. S. *Science (Washington, D.C.)* **1991**, *252*, 688–691. Chailapakul, O.; Crooks, R. M. *Langmuir* **1993**, *9*, 884–888.

(12) Rowe, G. K.; Creager, S. E. *Langmuir* **1991**, *7*, 2307–2312.

(13) For reviews, see: Bain, C. D.; Whitesides, G. M. *Angew. Chem., Int. Ed. Engl.* **1989**, *28*, 506–512. Whitesides, G. M.; Laibinis, P. E. *Langmuir* **1990**, *6*, 87–96. Ulman, A. *An Introduction to Ultrathin Organic Films From Langmuir-Blodgett to Self-Assembly*; Academic Press: San Diego CA, 1991; Chapter 3.

(14) Although mixed SAMs have not been systematically studied using the SEM, several recent studies have shown that the SEM can be used to detect lithographed patterns of different thiolates in SAM on small length scales; see: López, G. P.; Biebuyck, H. A.; Whitesides, G. M. *Langmuir* **1993**, *9*, 1513–1516. Wollman, E. W.; Frisbie, C. D.; Wrighton, M. S. *Langmuir* **1993**, *9*, 1517–1520. López, G. P.; Biebuyck, H. A.; Frisbie, C. D.; Whitesides, G. M. *Science (Washington D.C.)* **1993**, *260*, 647–649. Kumar, A.; Whitesides, G. M. *Appl. Phys. Lett.*, accepted for publication.

(15) A Monte Carlo simulation indicates that mixed SAMs containing mixtures of a thiolates with long chains ($-S(CH_2)_{19}CH_3$) and thiolates with short chains ($-S(CH_2)_9CH_3$) will phase separate on gold if allowed to equilibrate fully by lateral diffusion in the plane of the monolayer: Siepmann, J. I.; McDonald, I. R. *Mol. Phys.* **1992**, *75*, 255–259.

(16) In a recent study of the polymerization of styrene-*p*-sulfonate on ammonium-terminated monolayers, phase separation of two-component monolayers derived from an ammonium-terminated disulfide and a perfluorinated thiol was inferred from the inability of the mixed SAMs to block electron transfer between $Fe(CN)_6^{3-}$ in solution and the underlying gold electrode after polymerization: Niwa, M.; Mori, T.; Nigashi, N. *J. Mater. Chem.* **1992**, *2*, 245–251. In this study, the authors polymerized the styrene derivative on top of the SAMs using UV photoinitiation and examined the ability of the films to block electron transfer. When the mixed SAMs were used, they observed that increased photolysis decreased the ability of films to impede electron transfer. The results in another recent paper suggest that the observations of Niwa et al. may not be due to phase separation but rather to partial removal of the SAM by UV-promoted oxidation of the thiolate groups: Huang, J.; Hemminger, J. C. *J. Am. Chem. Soc.* **1993**, *115*, 3342–3343.

(17) Domains in phase-separated Langmuir-Blodgett films have been imaged using the atomic force microscope (AFM) and a frictional force microscope (FFM), a modification of an atomic force microscope. AFM: Chi, L. F.; Anders, M.; Fuchs, H.; Johnston, R. R.; Ringsdorf, H. *Science (Washington, D.C.)* **1993**, *259*, 213–216. FFM: Overney, R. M.; Meyer, E.; Frommer, J.; Brodbeck, D.; Luethi, R.; Howald, L.; Guentherodt, H. J.; Fuijihira, M.; Takano, H.; Gotoh, Y. *Nature (London)* **1992**, *359*, 133–135.

(18) Stranick, S. J.; Weiss, P. S.; Parikh, A. N.; Tao, Y.-T.; Allara, D. L., private communication.

(19) Häussling, L.; Michel, B.; Ringsdorf, H.; Rohrer, H. *Angew. Chem., Int. Ed. Engl.* **1991**, *30*, 569–572.

(20) Au: Nuzzo, R. G.; Allara, D. L. *J. Am. Chem. Soc.* **1983**, *105*, 4481–4483. Porter, M. D.; Bright, T. B.; Allara, D. L.; Chidsey, C. E. D. *J. Am. Chem. Soc.* **1987**, *109*, 3559–3568. Bain, C. D.; Troughton, E. B.; Tao, Y.-T.; Evall, J.; Whitesides, G. M.; Nuzzo, R. G. *J. Am. Chem. Soc.* **1989**, *111*, 321–335. Ag: Walczak, M. M.; Chung, C.; Stole, S. M.; Widrig, C. A.; Porter, M. D. *J. Am. Chem. Soc.* **1991**, *113*, 2370–2378. Cu, Ag, Au: Laibinis, P. E.; Whitesides, G. M.; Allara, D. L.; Tao, Y.-T.; Parikh, A. N.; Nuzzo, R. G. *J. Am. Chem. Soc.* **1991**, *113*, 7152–7167.

(21) Laibinis, P. E.; Fox, M. A.; Folkers, J. P.; Whitesides, G. M. *Langmuir* **1991**, *7*, 3167–3173.

(22) Transmission electron diffraction: Strong, L.; Whitesides, G. M. *Langmuir* **1988**, *4*, 546–558. Helium atom diffraction: Chidsey, C. E. D.; Liu, G.-Y.; Rowntree, P.; Scoles, G. *J. Chem. Phys.* **1989**, *91*, 4421–4423. Infrared spectroscopy: Nuzzo, R. G.; Korenic, E. M.; Dubois, L. H. *J. Chem. Phys.* **1990**, *93*, 767–773. Infrared spectroscopy and electron diffraction: Dubois, L. H.; Zegarski, B. R.; Nuzzo, R. G. *J. Chem. Phys.* **1993**, *98*, 678–688. X-ray diffraction: Samant, M. G.; Brown, C. A.; Gordon, J. G., II. *Langmuir* **1991**, *7*, 437–439. Fenter, P.; Eisenberger, P.; Li, J.; Camillone, N., III; Bernasek, S.; Scoles, G.; Ramanarayanan, T. A.; Liang, K. S. *Langmuir* **1991**, *7*, 2013–2016. Fenter, P.; Eisenberger, P.; Liang, K. S. *Phys. Rev. Lett.* **1993**, *70*, 2447–2450. Scanning tunneling microscopy: Widrig, C. A.; Alves, C. A.; Porter, M. D. *J. Am. Chem. Soc.* **1991**, *113*, 2805–2810. Atomic force

microscopy: Alves, C. A.; Smith, E. L.; Porter, M. D. *J. Am. Chem. Soc.* **1992**, *114*, 1222–1227.

(23) For studies on the structures and properties of monolayers with various tail groups, see: Nuzzo, R. G.; Dubois, L. H.; Allara, D. L. *J. Am. Chem. Soc.* **1990**, *112*, 558–569. Dubois, L. H.; Zegarski, B. R.; Nuzzo, R. G. *J. Am. Chem. Soc.* **1990**, *112*, 570–579. Chidsey, C. E. D.; Loiacono, D. N. *Langmuir* **1990**, *6*, 682–691.

(24) For molecular dynamics calculations on the structures and properties of single-component SAMs, see: Hautman, J.; Klein, M. L. *J. Chem. Phys.* **1989**, *91*, 4994–5001. Ulman, A.; Eilers, J. E.; Tillman, N. *Langmuir* **1989**, *5*, 1147–1152. Hautman, J.; Bareman, J. P.; Mar, W.; Klein, M. L. *J. Chem. Soc., Faraday Trans.* **1991**, *87*, 2031–2037. Hautman, J.; Klein, M. L. *Phys. Rev. Lett.* **1991**, *67*, 1763–1766.

(25) For a diffusion coefficient of 2×10^{-7} cm^2/s for a molecule in a Langmuir monolayer (determined electrochemically at 28 °C for the diffusion of *N*-octadecylferrocenecarboxamide at the air–water interface in a monolayer with a void volume of 4 Å^2/molecule; see: Charych, D. H.; Landau, E. M.; Majda, M. *J. Am. Chem. Soc.* **1991**, *113*, 3340–3346), molecules diffuse 0.1 μm in 250 μs.

(26) Phase-separated domains within Langmuir monolayers have been observed directly with the use of the epifluorescence microscope: Von Tscharner, V.; McConnell, H. M. *Biophys. J.* **1981**, *36*, 409–419. Lösche, M.; Sackmann, E.; Möhwald, H. *Ber. Bunsenges. Phys. Chem.* **1983**, *87*, 848–852. McConnell, H. M.; Tamm, L. K.; Weis, R. M. *Proc. Natl. Acad. Sci. U.S.A.* **1984**, *81*, 3249–3253. Weis, R. M.; McConnell, H. M. *Nature (London)* **1984**, *310*, 47–49. Heckl, W. M.; Möhwald, H. *Ber. Bunsenges. Phys. Chem.* **1986**, *90*, 3249–3253. Chi, L. F.; Johnston, R. R.; Ringsdorf, H. *Langmuir* **1991**, *7*, 2323–2329.

(27) Phase separation has been inferred for two-component Langmuir films containing a phosphatidylcholine and a small mole fraction of cholesterol. For examples, see: Pagano, R. E.; Gershfeld, N. L. *J. Phys. Chem.* **1972**, *76*, 1238–1243. Gershfeld, N. L.; Pagano, R. E. *J. Phys. Chem.* **1972**, *76*, 1244–1249. Tajima, K.; Gershfeld, N. L. in *Monolayers*; Goddard, E. D.; Ed.; ACS Advances in Chemistry Series 144; American Chemical Society: Washington D.C., 1975; pp 165–176. Subramaniam, S.; McConnell, H. M. *J. Phys. Chem.* **1987**, *91*, 1715–1719. Heckl, W. M.; Cadenhead, D. A.; Möhwald, H. *Langmuir*, **1988**, 1352–1358. Rice, P. A.; McConnell, H. M. *Proc. Natl. Acad. Sci. U.S.A.* **1989**, *86*, 6445–6448.

(28) Although the lateral diffusion coefficients for self-assembled monolayers of alkanethiolates on gold have not been determined experimentally, lines of alkanethiolate on gold as small as 0.10 μm wide show no evidence of spreading over a period of several hours at scales of 0.1 μm (Abbott, N. L.; Biebuyck, H. A.; Kumar, A.; Lopez, G. P.; Whitesides, G. M., unpublished observations). From comparisons of these observations with those characterizing the lateral diffusion coefficients in Langmuir monolayers,[25] we infer that lateral diffusion is probably not the predominant mechanism of equilibration in mixed SAMs of alkanethiolates on gold.

(29) In a recent study, self-assembled monolayers derived from octadecanethiol were used as masks for lithography with the scanning tunneling microscope (STM). Pits with dimensions of 25 nm × 25 nm were etched in the monolayer with the STM; these pits "were dimensionally stable for at least several days", implying that lateral diffusion of the thiolates on the gold is very slow (unless the etched areas were damaged during the etching process): Ross, C. B.; Sun, L.; Crooks, R. M. *Langmuir* **1993**, *9*, 632–636.

(30) In ref 5, mixed SAMs were formed at room temperature from solutions containing mixtures of $HS(CH_2)_{21}CH_3$ and $HS(CD_2)_{11}CD_3$ and solutions containing mixtures of $HS(CD_2)_{17}CD_3$ and $HS(CH_2)_{11}CH_3$. Since these components have lengths similar to those used in the present study, we would expect their behavior to be analogous to the behavior of the SAMs formed under similar conditions in this study.

(31) The morphology of the gold substrates should affect the properties of a SAM and may affect the distribution of thiolates in mixed SAMs that have not reached equilibrium. In this study we used substrates formed by the evaporation of gold onto silicon wafers that had been primed with 100 Å of chromium as an adhesion layer between the gold and the oxide layer on the silicon. Substrates formed under these conditions consist of mounds of gold that are approximately 100 nm across and 20–30 nm high.[4]

(32) Topology could affect the rate of exchange between thiolates in the SAM and thiols in solution. Annealing the gold during (or after) evaporation can lead to gold substrates with smoother topologies: Hallmark, V. M.; Chiang, S.; Rabolt, J. F.; Swalen, J. D.; Wilson, R. J. *Phys. Rev. Lett.* **1987**, *59*, 2879–2882. Chidsey, C. E. D.; Loiacono, D. N.; Sleator, T.; Nakahara, S. *Surf. Sci.* **1988**, *200*, 45–66. Putnam, A.; Blackford, B. L.; Jericho, M. H.; Watanabe, M. O. *Surf. Sci.* **1989**, *217*, 276–288. Vancea, J.; Reiss, G.; Schneider, F.; Bauer, K.; Hoffmann, H. *Surf. Sci.* **1989**, *218*, 108–126.

(33) Exchange between thiolates in the SAM and thiols in solution is slower for SAMs formed on gold substrates that were etched with *aqua regia* prior to formation of the SAM than on similar substrates that were not etched; this effect was attributed to a lower number of defects in the etched gold substrates: Creager, S. E.; Hockett, L. A.; Rowe, G. K. *Langmuir* **1992**, *8*, 854–861.

(34) Examples of studies showing the diffusion of atoms of Au on annealed surfaces: Jaklevic, R. C.; Elie, L. *Phys. Rev. Lett.* **1988**, *60*, 120–123. Emch, R.; Nogami, J.; Dovek, M. M.; Lang, C. A.; Quate, C. F. *J. Appl. Phys.* **1989**, *65*, 79–84. Trevor, D. J.; Chidsey, C. E. D.; Loiacono, D. N. *Phys. Rev. Lett.* **1989**, *62*, 929–932. Sommerfeld, D. A.; Cambron, R. T.; Beebe, T. P., Jr. *J. Phys. Chem.* **1990**, *94*, 8926–8932. Holland-Moritz, E.; Gordon, J., II; Borges, G.; Sonnenfeld, R. *Langmuir* **1991**, *7*, 301–306. Gimzewski, J. K.; Berndt, R.; Schlittler, R. R. *Phys. Rev. B* **1992**, *45*, 6844–6857.

(35) Weiss, P. S.; Allara, D. L., private communication.

(36) We have determined the "completeness" of a SAM from the difference in the thickness between the two single-component SAMs as determined using XPS.[4,5]

(37) If we leave the gold substrates in these solutions for longer than 1 h, the SAMs begin to favor the longer component and the transition region begins to sharpen.

(38) When $R_{soln} > \sim 0.2$, the monolayer is composed largely of the longer component ($\chi_{Lg,SAM} \approx 1$); when $R_{soln} < 0.07$, the SAMs are composed largely of the shorter component ($\chi_{Lg,SAM} \approx 0$).

(39) The individual sets of data in Figure 1c for $[RSH]_T = 1$ mM and $[RSH]_T = 10$ mM are considerably sharper than the two sets appear to be when combined. We combined the two sets because they were close enough to believe that the difference was only due to a difference in the preparation of the solutions.

(40) We have not included data for SAMs for at room temperature with $[RSH]_T = 1$ μM because after 1 day all of the SAMs had not formed completely enough to give a consistent set of XPS data.

(41) Folkers, J. P.; Laibinis, P. E.; Whitesides, G. M. *J. Adhes. Sci. Technol.* **1992**, *6*, 1397–1410.

(42) Hysteresis in contact angles remains a poorly understood phenomenon, although it is commonly attributed to the chemical heterogeneity and roughness of an interface. For a conceptual review of contact angles and hysteresis, see: de Gennes, P. G. *Rev. Mod. Phys.* **1985**, *57*, 827–863. For other studies on hysteresis, see: Johnson, R. E., Jr.; Dettre, R. H. In *Contact Angle, Wettability, and Adhesion*; Gould, R. F., Ed.; ACS Advances in Chemistry Series 43; American Chemical Society: Washington, D.C., 1964; pp 112–135. Dettre, R. H.; Johnson, R. E., Jr. In *Contact Angle, Wettability, and Adhesion*; Gould, R. F., Ed.; ACS Advances in Chemistry Series 43; American Chemical Society: Washington, D.C., 1964; pp 136–144. Joanny, J. F.; de Gennes, P. G. *J. Chem. Phys.* **1984**, *81*, 552–562. Schwartz, L. W.; Garoff, S. *Langmuir*, **1985**, *1*, 219–230. Andrade, J. D.; Smith, L. M.; Gregonis, D. E. In *Surface and Interfacial Aspects of Biomedical Polymers*; Andrade, J. D., Ed.; Plenum Press: New York, 1985; Vol. 1, pp 249–292. Chen, Y. L.; Helm, C. A.; Israelachvili, J. N. *J. Phys. Chem.* **1991**, *95*, 10736–10747.

(43) We have not eliminated the possibility that the exchange processes are roughening the surfaces by dissolution of gold atoms on the surface. A recent study using the scanning tunneling microscope has shown that gold surfaces are roughened after exposure to thiol from ethanol. Gold was also detected in the solution after adsorption for 24 h; the amount of gold found in solution corresponded to approximately 50% of a monolayer: Edinger, K.; Gölzhäuser, A.; Demota, K.; Wöll, Ch.; Grunze, M. *Langmuir* **1993**, *9*, 4–8.

(44) Bragg, W. L.; Williams, E. J. *Proc. R. Soc. London* **1936**, *145*, 699–730.

(45) The Bragg–Williams approximation has been used to model the adsorption isotherms of single- and two-component gases and surfactants. For examples, see: Jaroniec, M.; Piotrowska, J. *Colloid Polymn. Sci.* **1980**, *258*, 977–979. Retter, U. *J. Electroanal. Chem.* **1987**, *236*, 21–30. Cases, J. M.; Villieras, F. *Langmuir* **1992**, *8*, 1251–1264.

(46) In eqs 2 and 3 we are making the approximation that the mole fractions of the component in solution and in the SAM and their activities are the same—that is, we are assuming activity coefficients of 1.

(47) This "standard state" is for theoretical purposes only. It is a common standard state used for solutes because it extrapolates the chemical potential of the solute to infinite dilution rather than to the pure state, which would not be related to its chemical potential as a solute. The general equation for this standard state is

$$\mu^{\dagger}_{solute} = \lim_{y_{solvent} \to 1} (\mu^{soln}_{solute} - kT \ln y_{solute})$$

For further explanation, see: Kirkwood, J. G.; Oppenheim, I. *Chemical Thermodynamics*; McGraw-Hill: New York, 1961; Chapter 11.

(48) As long as both the reference and mixed SAMs are complete (see Scheme I), we are working at a constant pressure within the monolayers. Following the formalism developed for monolayers at the air–water interface, the enthalpy and internal energy are effectively equal as long as we assume that the change in pressure upon mixing is zero. For examples of the equation of state for two-component, insoluble monolayers at the air–water interface, see: Lucassen-Reynders, E. H. *J. Colloid Interface Sci.* **1972**, *41*, 156–167. Gaines, G. L., Jr. *J. Chem. Phys.* **1978**, *69*, 924–930. Adamson, A. *Physical Chemistry of Surface*, 4th ed.; Wiley: New York, 1982; pp 139–143 and references therein.

(49) The values of $R^{SAM=1}_{soln}$ in ref 4 were determined on systems that were not at equilibrium. We therefore cannot relate those values to $\Delta(\Delta\mu)$.

(50) Folkers, J. P.; Whitesides, G. M., unpublished observations.

(51) Nuzzo, R. G.; Zegarski, B. R.; Dubois, L. H. *J. Am. Chem. Soc.* **1987**, *109*, 733–740.

(52) Troughton, E. B.; Bain, C. D.; Whitesides, G. M.; Nuzzo, R. G.; Allara, D. L.; Porter, M. D. *Langmuir* **1988**, *4*, 365–385.

(53) Several warnings have recently appeared concerning "piranha solution": Dobbs, D. A.; Bergman, R. G.; Theopold, K. H. *Chem. Eng. News* **1990**, *68* (17), 2. Wnuk, T. *Chem. Eng. News* **1990**, *68* (26), 2. Matlow, S. L. *Chem. Eng. News* **1990**, *68* (30), 2.

(54) Bain, C. D.; Whitesides, G. M. *J. Phys. Chem.* **1989**, *93*, 1670–1673.

(55) Laibinis, P. E.; Bain, C. D.; Whitesides, G. M. *J. Phys. Chem.* **1991**, *95*, 7017–7021.